

Article

Light and Airy: A Simple Solution for Relativistic Quantum Acceleration Radiation

Michael R. R. Good ^{1,2*}  and Eric V. Linder ^{2,3} ¹ Physics Department, Nazarbaev University, Nur-Sultan 010000, Kazakhstan² Energetic Cosmos Laboratory, Nazarbayev University, Nur-Sultan 010000, Kazakhstan; evlinder@lbl.gov³ Berkeley Center for Cosmological Physics & Berkeley Lab, University of California, Berkeley, CA 94720, USA* Correspondence: michael.good@nu.edu.kz

Abstract: We study the quantum radiation of particle production by vacuum from an ultra-relativistic moving mirror (dynamical Casimir effect) solution that allows (possibly for the first time) analytically calculable time evolution of particle creation and an Airy particle spectral distribution. The reality of the beta Bogoliubov coefficients is responsible for the simplicity, and the mirror is asymptotically inertial at the speed of light, with finite energy production. We also discuss general relations regarding negative energy flux, the transformation to the 1-D Schrödinger equation, and the incompleteness of entanglement entropy.

Keywords: moving mirrors; acceleration radiation; black holes; quantum field theory in curved space



Citation: Good, M.R.R.; Linder, E.V. Light and Airy: A Simple Solution for Relativistic Quantum Acceleration Radiation. *Universe* **2021**, *7*, 60. <https://doi.org/10.3390/universe7030060>

Academic Editor: Galina L. Klimchitskaya

Received: 11 February 2021
Accepted: 4 March 2021
Published: 5 March 2021

Publisher's Note: MDPI stays neutral with regard to jurisdictional claims in published maps and institutional affiliations.



Copyright: © 2021 by the authors. Licensee MDPI, Basel, Switzerland. This article is an open access article distributed under the terms and conditions of the Creative Commons Attribution (CC BY) license (<https://creativecommons.org/licenses/by/4.0/>).

1. Introduction

The dynamical Casimir effect (DCE) [1–4] is a celebrated and multidisciplinary phenomena that plays an important role in many areas of physics ranging from quantum fields, atomic physics, condensed matter, and applications in nanotechnology all the way to astrophysics, cosmology and gravitation. The overarching reach of the DCE results from the fact that it is sourced, like the Unruh effect [5], by the amplified zero-point fluctuations of quantized fields, inherent to physical systems. Notable theoretical studies [6–8] have helped lead to experiments (the first being [9]) which have been successful at verifying the existence of the DCE (see a pedagogical overview here: [10]). The quantum acceleration radiation of the DCE is well-connected to the Hawking effect [11], potentially bringing experimental data to bear on the quantum relationship between gravity and acceleration.

Studying acceleration radiation with finite energy production is physically well-motivated. In the case of black hole evaporation, for example, this is a conspicuous sign that the evolution has finished, energetic radiation has stopped, and conservation of energy is upheld. The canonical moving mirror model of DeWitt–Davies–Fulling [2–4], for a single perfectly reflecting boundary point in flat (1+1)-D spacetime, has solutions demonstrating in a simple way total finite energy production (e.g., the four decade old solution of Walker–Davies which first derived a finite amount of energy creation [12]). Recently, several finite energy mirror solutions have been found that demonstrate close connections to strong gravitational systems. These gravity analog models are called accelerated boundary correspondences (ABCs). The infinite energy ABC solutions correspond to the most well-known spacetimes, e.g., Schwarzschild [13], Reissner–Nordström (RN) [14], Kerr [15], and de Sitter [16]. The finite energy ABC solutions closely characterize interesting well-known curved spacetime end-states, including extremal black holes (asymptotic uniformly accelerated mirrors [15,17–20]), black hole remnants (asymptotic constant-velocity mirrors [21–26]) and complete black hole evaporation (asymptotic zero-velocity mirrors [12,27–32]).

Despite this progress, it has been very hard to find a mirror solution whose particle spectrum is simple. Only two known solutions have analytic forms, one whose spectrum

is an infinite sum of terms [26] and another which is so lengthy as to be prohibitively cumbersome [27,28]. Consequently, analytic time evolution is impossible to find for the above spectra. Further investigation of the particle production at any given moment is hobbled because one must instead resort to numerical analysis and finite sized frequency-time bins utilizing the discrete nature of orthonormal wave packets [30].

Motivated by simplicity, we take a step back and consider that any Bogoliubov transformation can be broken down into two types: (1) the trivial unitary transformation with β Bogoliubov coefficient zero, $\beta = 0$, indicating no particle production and (2) squeezing transformations where the $\beta \neq 0$ is given by a transformation matrix that is diagonal [33] (see the Bloch-Messiah decomposition or the theory of singular values). The simplest examples of the non-trivial transformations are those where the Bogoliubov coefficients are *real-valued*. We therefore look for some mirror motion (i.e., ABC) that should lead to a real non-zero beta Bogoliubov coefficient for particle creation, and anticipate corresponding simplicity in the resulting spectrum.

We take the simplest possible choice for global mirror motion with characteristics leading to the desired reality of the Bogoliubov coefficient, and indeed find a simple solution for the particle production spectrum. Remarkably, a transformation to the time domain on this spectrum analytically gives the particle production at any given moment.

Our paper is organized as follows: in Section 2 we give a very brief motivation of the connection between the reality of the beta Bogoliubov coefficient and the mirror trajectory properties. We analyze this accelerated trajectory in Section 3, computing the key relativistic dynamical properties such as rapidity, speed, and acceleration. In Section 4, we derive the energy radiated, by analysis of the quantum stress tensor, and in Section 5 we derive the particle spectrum, finding a unique Airy-Ai form for the radiation and confirming consistency with the stress tensor results. Finally, in Section 6 we compute the time evolution of particle creation analytically. Appendices A and B discuss some general properties leading to necessary negative energy flux, and connecting to the 1-D Schrödinger equation, respectively. Appendix C is a note on the connection between rapidity and entanglement entropy. Throughout we use natural units, $\hbar = c = 1$.

2. Reality, Acceleration, and Inertia

The beta Bogoliubov coefficient controls quantum particle production and to compute it, we need the trajectory of the mirror. Mirror motions can be written in configuration space, (x, t) , but also in light-cone (null) coordinates (u, v) . Here retarded time is $u = t - x$ and advanced time is $v = t + x$, while the moving mirror trajectory $f(v)$ gives retarded time location, where u is switched out for f since u is the independent variable and f is the trajectory function. The beta Bogoliubov coefficient is [34]

$$\beta_{\omega\omega'} = \frac{-1}{4\pi\sqrt{\omega\omega'}} \int_{-\infty}^{+\infty} dv s. e^{-i\omega'vs - i\omega f(v)} (\omega f'(v) - \omega'), \tag{1}$$

where ω and ω' are the frequencies of the outgoing and incoming modes, respectively, [35].

To maintain finite energy and the simplicity of no information loss, there must not be a horizon at finite time, and the acceleration must vanish at infinity (i.e., the mirror motion must be asymptotically inertial). Under these conditions we can carry out an integration by parts to give

$$\beta_{\omega\omega'} = \frac{1}{2\pi} \sqrt{\frac{\omega'}{\omega}} \int_{-\infty}^{+\infty} dv e^{-i\omega'v - i\omega f(v)}. \tag{2}$$

To guarantee a real-valued beta Bogoliubov coefficient, the mirror trajectory $f(v)$ must be an odd function so that the exponential over the symmetric interval turns into a cosine of the argument, i.e., a real valued function. The simplest odd function that accelerates in the required manner is $f(v) \sim vs. + v^3$. We will find this results in not only interesting dynamics, but analytic calculation of particle production spectrum and time evolution.

3. Trajectory Motion

As motivated in the previous section, we expect the accelerated mirror trajectory

$$f(v) = vs. + \kappa^2 \frac{v^3}{3}, \tag{3}$$

to have interesting physical properties. Here κ is a quantity related to the acceleration (and the surface gravity in the black hole case).

We can also write the trajectory in spacetime coordinates,

$$t = -x + \frac{1}{\kappa}(-6\kappa x)^{1/3}, \tag{4}$$

taking the real cube root, or

$$x = -t - \frac{1}{2\kappa} \left[A_+^{2/3} A_-^{1/3} + A_+^{1/3} A_-^{2/3} \right], \tag{5}$$

where

$$A_{\pm} = 3\kappa t \pm \sqrt{9\kappa^2 t^2 + 8}. \tag{6}$$

Note at late times $x \rightarrow -t + \mathcal{O}(t^{1/3})$. These forms make it obvious that asymptotically the mirror travels at the speed of light.

A spacetime plot with time on the vertical axis is given of the trajectory in Figure 1. A conformal diagram is plotted in Figure 2. We next investigate the dynamics of the trajectory Equation (3).

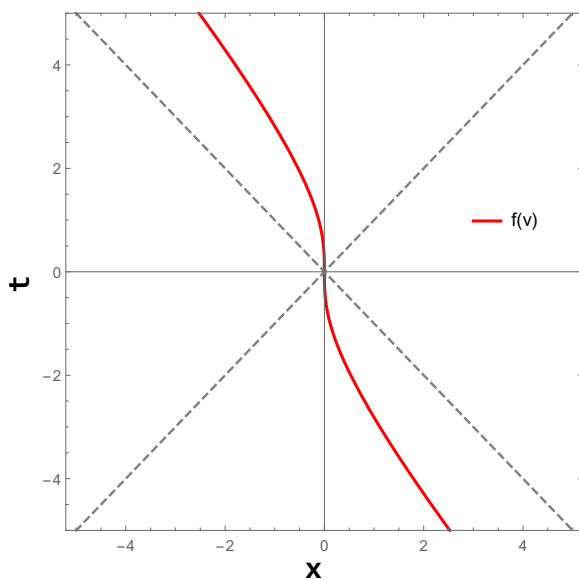


Figure 1. A spacetime diagram of the mirror trajectory, Equation (3) with $\kappa = 1$. It starts off asymptotically inertial with zero acceleration and light-speed velocity and decelerates, eventually reaching zero speed (at $t = 0$), and then accelerates again approaching the speed of light in an asymptotically inertial way. Note that field modes moving to the left will always hit the mirror, demonstrating no horizon, despite the mirror accelerating to light-speed.

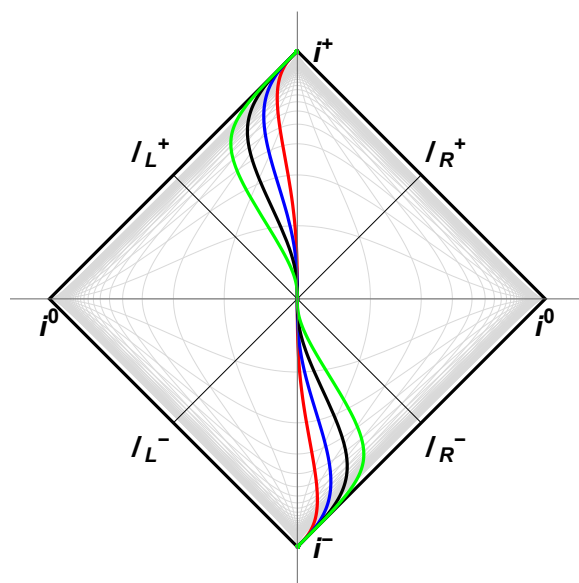


Figure 2. A Penrose diagram of the mirror trajectory, Equation (3). The mirror is moving at light-speed at $v \rightarrow \pm\infty$. Since the acceleration is asymptotically zero as $v \rightarrow \pm\infty$ then this mirror is asymptotically inertial. The various colors correspond to different maximum accelerations; here $\kappa = 1, 4, 16, 64$ from red, blue, black, and green.

We compute the rapidity $\eta(v)$ by $2\eta(v) \equiv -\ln f'(v)$ where the prime is a derivative with respect to the argument,

$$\eta(v) = -\frac{1}{2} \ln(\kappa^2 v^2 + 1). \tag{7}$$

From the rapidity we may easily compute the velocity $V \equiv \tanh \eta$, plugging in Equation (7),

$$V(v) = -\tanh\left[\frac{1}{2} \ln(\kappa^2 v^2 + 1)\right] = \frac{-\kappa^2 v^2}{2 + \kappa^2 v^2}, \tag{8}$$

and the proper acceleration, which follows from $\alpha(v) \equiv e^{\eta(v)} \eta'(v)$,

$$\alpha(v) = -\frac{\kappa^2 v}{(\kappa^2 v^2 + 1)^{3/2}}. \tag{9}$$

At $x = t = 0 = v$, the velocity and acceleration are zero. At asymptotic infinity, the velocity is the speed of light and the acceleration goes to zero. The magnitude of the velocity, Equation (8), along with the proper acceleration, Equation (9), are plotted in Figure 3. Often, an asymptotically initial zero velocity state is more common. Trajectories are normally either globally defined or piece-wise defined where the accelerated piece is glued to the static piece at the origin. Thus, the asymptotic light-speed property distinguishes the Airy trajectory Equation (3). However, what does it mean to start inertial at the speed of light? What exactly is the initial state of the system? Recall that the ‘mirror’ in the moving mirror model is a massless boundary condition imposed on the fields such that the modes are always zero at it. To start inertial is to start time-like, physically well-associated with familiar world-lines (which are by definition, time-like). The modes in the initial vacuum state are the usual plane wave form as is familiar from ordinary quantum field theory in Minkowski space. The only difference here is that the initial asymptotic inertial state of motion saturates the speed limit and pushes the model to its extreme, but causal effects on the field are still in the past light cone of the ‘reflection’ events that disturb the quantum field and amplify zero-point fluctuations. Cause and effect are still contiguously mediated across the flat spacetime.

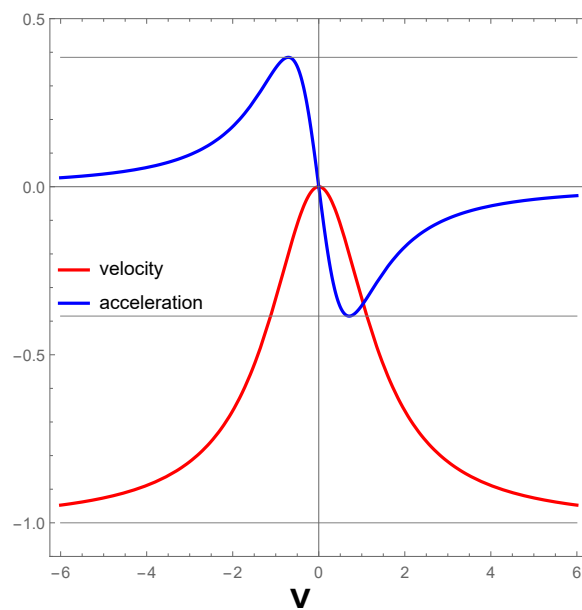


Figure 3. The velocity and proper acceleration as a function of light-cone coordinate advanced time $v = t + x$ for the mirror trajectory, Equation (3). At $v = 0$, the velocity $V = 0$, but asymptotically $|V| \rightarrow 1$ and the proper acceleration vanishes, $\alpha \rightarrow 0$. The maximum acceleration occurs at $|\alpha_{\max}| = 2\kappa/(3\sqrt{3}) = 0.385\kappa$. Here v is in units of $1/\kappa$ and the maximum accelerations happen at advanced time $\kappa v_{s.} = \pm 1/\sqrt{2} = 0.707$.

4. Energy Flux and Total Energy

4.1. Energy Flux

The quantum stress tensor reveals the energy flux emitted by the moving mirror. Typically, one will see [3]

$$F(u) = -\frac{1}{24\pi} \{p(u), u\}, \tag{10}$$

where the energy flux, $F(u)$, is a function of light-cone coordinate retarded time $u = t - x$ [4,34] and the brackets define the Schwarzian derivative. The trajectory in light-cone coordinates of the mirror is $p(u)$ which is the advanced time position “ v ” as a function of retarded time u . However, since we want advanced time v as the independent variable, we write the radiated energy flux using $f(v)$ [16,21],

$$F(v) = \frac{1}{24\pi} \{f(v), v\} f'(v)^{-2}, \tag{11}$$

where the Schwarzian brackets are defined as usual,

$$\{f(v), v\} \equiv \frac{f'''}{f'} - \frac{3}{2} \left(\frac{f''}{f'} \right)^2. \tag{12}$$

For $f(v)$ given by Equation (3), this yields

$$F(v) = \frac{\kappa^2}{12\pi} \frac{1 - 2\kappa^2 v^2}{(\kappa^2 v^2 + 1)^4}. \tag{13}$$

It is clear that asymptotically $F(v) \rightarrow 0$ for both $v \rightarrow \pm\infty$. Figure 4 shows the energy flux as a function of advanced time v .

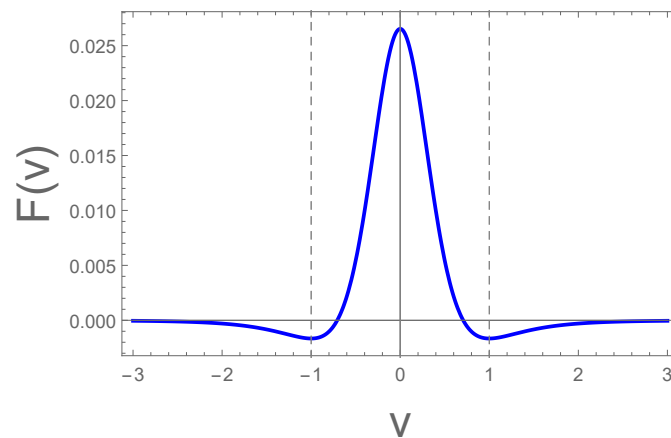


Figure 4. The energy flux, Equation (13), is asymptotically zero at $v = \pm\infty$. The total energy, as we shall see in Equation (16), is therefore finite, $E = \kappa/96$. Notice the emission of negative energy flux near early and late advanced times. The maximum flux $F_{\max} = \kappa^2/(12\pi)$ occurs at $v = 0$ and the minimum flux $F_{\min} = -\kappa^2/(192\pi)$ occurs at $v = \pm 1/\kappa$. The energy flux crosses zero, $F = 0$, at $v = \pm 1/(\sqrt{2}\kappa)$. Here $\kappa = 1$.

4.2. Total Energy

The total energy measured by a far away observer at \mathcal{S}_R^+ is [36]

$$E = \int_{-\infty}^{\infty} F(u) du, \tag{14}$$

where integration occurs over retarded time (it takes the energy time to reach \mathcal{S}_R^+). Since we are using advanced time v , we write this with $du = \frac{df}{dv} dv$ to get the Jacobian correct,

$$E = \int_{-\infty}^{+\infty} F(v) f'(v) dv. \tag{15}$$

Plugging in Equations (3) and (13) into Equation (15), with Jacobian $du/dv = \kappa^2 v^2 + 1$, the simple result is

$$E = \frac{\kappa}{96}, \tag{16}$$

which is finite and positive.

Physically, the finite value tells us the evaporation process stops, similar to the ABC’s of extremal black holes (asymptotic uniformly accelerated mirrors), black hole remnants (non-horizon sub-light-speed asymptotic coasting mirrors), and complete black hole evaporation (asymptotic static moving mirrors). The fact that the total energy is positive is consistent with the quantum interest conjecture [37] as derived from quantum inequalities [38].

4.3. Negative Energy Flux

As seen from Figure 4, there are regions of negative energy flux (NEF). This is required by the unitarity sum rule (see Appendices A and B and, e.g., [27]). These regions extend for $|v| > 1/(\kappa\sqrt{2})$. The total negative energy is, by symmetry,

$$E_{NEF} = 2 \int_{v=+\frac{1}{\kappa\sqrt{2}}}^{v=+\infty} F(v) f'(v) dv, \tag{17}$$

which gives an analytic result

$$E_{NEF} = \frac{\kappa(-10\sqrt{2} + 3\pi - 6 \cot^{-1} \sqrt{2})}{288\pi} = -0.00930\kappa \tag{18}$$

As a ratio, the emission of NEF to positive energy flux (PEF) is

$$\frac{|E_{NEF}|}{E_{PEF}} \approx 47.1\% . \tag{19}$$

Note one cannot judge by eye this ratio in Figure 4 due to the redshift Jacobian $f'(v)$ in Equation (17).

The NEF is a result of asymptotic inertia. We point out that the asymptotic inertia, while ensuring the total energy is finite, does not ensure information preservation [39]. Only the absence of a horizon guarantees that. In the Airy case, even though there is no horizon, and thus no information loss, the entanglement entropy diverges. This is because the rapidity diverges, as seen through the relationship $S = -\eta/6$. This indicates that entanglement entropy is not a comprehensive measure of the unitary, finite energy, information preserving dynamics, due to the inertial light speed asymptote (see Appendix C for more detail).

5. Particle Spectrum

The particle spectrum can be obtained from the beta Bogoliubov coefficient, given by Equation (2) in Section 2. For the particular trajectory Equation (3), as promised the Bogoliubov coefficient is real,

$$\beta_{\omega\omega'} = \frac{-1}{(\omega\kappa^2)^{1/3}} \sqrt{\frac{\omega'}{\omega}} \text{Ai}\left(\frac{\omega + \omega'}{(\omega\kappa^2)^{1/3}}\right), \tag{20}$$

which is highly unusual. This corresponds to the Bogoliubov transformation being a pure boost without rotation, i.e., there is no phase on the beta coefficient, giving us a natural choice for both field modes and coefficients (and potentially an action integral whose real part defines the vacuum–vacuum amplitude [40]).

To obtain the particle spectrum, we take the modulus square, $N_{\omega\omega'} \equiv |\beta_{\omega\omega'}|^2$, which gives

$$N_{\omega\omega'} = \frac{\omega'}{\kappa^{4/3}\omega^{5/3}} \text{Ai}^2\left(\frac{\omega + \omega'}{\kappa^{2/3}\omega^{1/3}}\right). \tag{21}$$

The Airy-Ai function is perhaps most well-known as the solution to the time-independent Schrödinger equation for a particle confined within a triangular potential well and for a particle in a one-dimensional constant force field. The spectrum Equation (21), $|\beta_{\omega\omega'}|^2$, is explicitly non-thermal and plotted as a contour plot in Figure 5.

This demonstrates a new spectrum of radiation emanating from a moving mirror trajectory. Equation (21) can be compared to the late time (equilibrium after formation) spectra of non-extremal black holes (e.g., Schwarzschild, RN, Kerr),

$$N_{\omega\omega'} = \frac{1}{2\pi\kappa\omega'} \frac{1}{e^{2\pi\omega/\kappa} - 1}, \tag{22}$$

and extremal black holes (e.g., extremal RN, extremal Kerr, extremal Kerr-Newman),

$$N_{\omega\omega'} = \frac{e^{-\pi\omega c/\mathcal{A}}}{\pi^2 \mathcal{A}^2} \left| K_{1+i\omega c/\mathcal{A}}\left(\frac{2}{\mathcal{A}}\sqrt{\omega\omega'}\right) \right|^2. \tag{23}$$

(For extremal Kerr, $c = \sqrt{2}$; for extremal RN, $c = 2$; for extremal Kerr-Newman, $c = \mathcal{A}/\kappa$.) Here κ is the surface gravity, i.e., $\kappa = 1/(4M)$ in the case of a Schwarzschild black hole, or outer horizon surface gravity for the RN and Kerr non-extremal black holes. In addition, \mathcal{A} is the extremal parameter, or the asymptotic uniform acceleration [20] in the case of the mirror system, while K_ν is the modified Bessel function of the second kind with order ν .

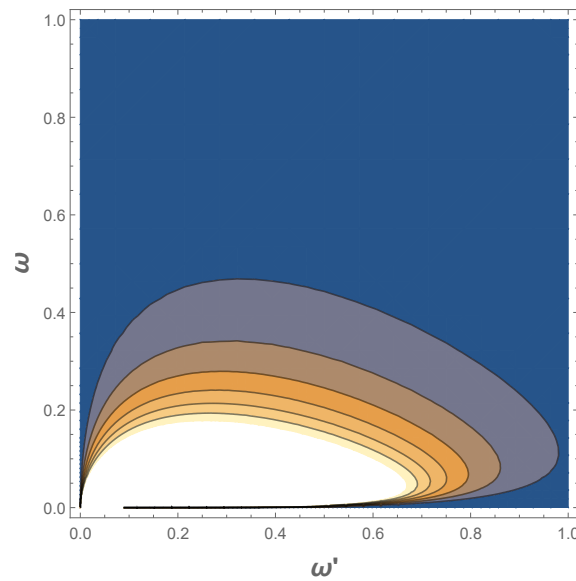


Figure 5. The Airy-Ai spectrum, $|\beta_{\omega\omega'}|^2$ from Equation (21), as a contour plot, here with $\kappa = 1$. The brighter the contours the more particle production. Notice the asymmetry between ω and ω' which are uniformly scaled. This asymmetry ultimately shows up in the infinite total particle count due to the infrared divergence of ω in N_ω but makes it possible to analytically integrate $N_{\omega\omega'}$ over ω' .

Furthermore, it is remarkable that the spectrum

$$N_\omega = \int_0^\infty N_{\omega\omega'} d\omega', \tag{24}$$

is analytic,

$$N_\omega = \frac{2\sqrt{\bar{\omega}}}{3\kappa} \text{Ai}^2(\bar{\omega}) - \frac{\text{Ai}(\bar{\omega})\text{Ai}'(\bar{\omega})}{3\kappa\bar{\omega}^{3/2}} - \frac{2\text{Ai}'^2(\bar{\omega})}{3\kappa\sqrt{\bar{\omega}}}, \tag{25}$$

where $\bar{\omega} \equiv (\omega/\kappa)^{2/3}$. This analytic $N(\omega)$ spectrum is plotted in Figure 6 for all κ .

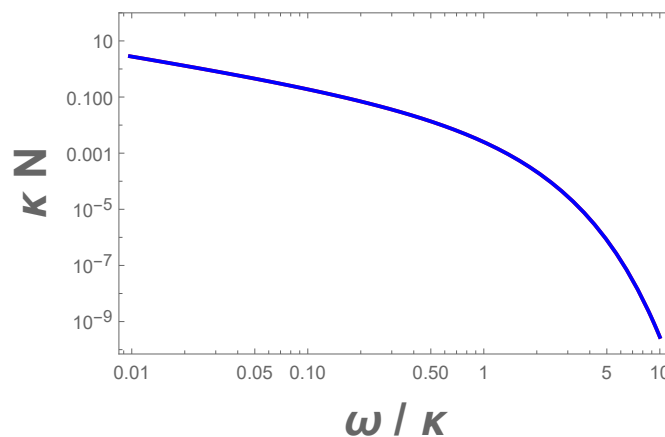


Figure 6. The Airy particle spectrum, $N(\omega)$, Equation (25). Note the infrared divergence at $\omega \rightarrow 0$; the soft particle divergence results in infinite total particle count characteristic of asymptotic coasting mirrors. Larger maximum acceleration as measured by κ results in more particles for a wider range of frequencies, i.e., N scales as $1/\kappa$ as seen by the κN curve plotted vs. ω/κ .

The Airy functions can be reformulated into Bessel functions using the identities

$$\text{Ai}(x) = \sqrt{\frac{x}{3\pi^2}} K_{1/3}\left(\frac{2}{3}x^{3/2}\right) \tag{26}$$

$$\text{Ai}'(x) = \frac{-x}{\sqrt{3\pi^2}} K_{2/3}\left(\frac{2}{3}x^{3/2}\right). \tag{27}$$

This turns Equation (21) into

$$N_{\omega\omega'} = \frac{1}{3\pi^2\kappa^2} \frac{q'(q+q')}{q^2} K_{1/3}^2\left(\frac{2(q+q')^{3/2}}{3q^{1/2}}\right), \tag{28}$$

which has similarities to the extremal black hole expression. Here $q = \omega/\kappa, q' = \omega'/\kappa$. For the particle spectrum we get

$$9\pi^2\kappa N_{\omega} = 2qK_{1/3}^2(2q/3) + K_{1/3}(2q/3) K_{2/3}(2q/3) - 2qK_{2/3}^2(2q/3). \tag{29}$$

In the small and large ω limits the leading order terms are, respectively,

$$N_{\omega} \rightarrow \frac{1}{6\sqrt{3}\pi\omega}, \quad \omega \rightarrow 0, \tag{30}$$

$$\rightarrow \frac{\kappa}{16\pi\omega^2} e^{-4\omega/(3\kappa)}, \quad \omega \rightarrow \infty. \tag{31}$$

The $1/\omega$ in the small frequency limit (note this is independent of κ) demonstrates the infrared divergence leading to an infinite total particle count commonly associated with constant-velocity moving mirror solutions [21–26], that are not asymptotically static (asymptotic zero-velocity [12,27–32]).

To check that the energy is indeed carried away by the particles, we look for consistency between Equation (21) and the total energy, Equation (16), found from the stress tensor. This is done by quantum summing,

$$E = \int_0^\infty \int_0^\infty \omega N_{\omega\omega'} d\omega d\omega', \tag{32}$$

that is, associating a quantum of energy ω with the particle distribution and integrating over all the frequencies. The result is pleasingly analytic:

$$E = \frac{\kappa}{96}. \tag{33}$$

Since this is also the result of Equation (16), the beta spectrum Equation (21), or Equation (29), is consistent with the quantum stress tensor, Equation (13).

The time dependence of particle creation can be computed via wavepacket analysis treated in Hawking [11], and explicitly numerically computed in [27,28]. Wave packet localization, particularly via orthonormal and complete sets in the moving mirror model, was first carried out in detail in [41]. For completeness, we utilize the same code to illustrate particle creation in time and present the results in Figure 7. The rate of emission of particles is finite only in a given time and frequency interval which can be seen by these complete orthonormal family of wave packets constructed from the beta Bogoliubov coefficients, following Hawking’s notation,

$$\beta_{jn\omega'} = \frac{1}{\sqrt{\epsilon}} \int_{j\epsilon}^{(j+1)\epsilon} d\omega e^{2\pi i\omega n/\epsilon} \beta_{\omega\omega'}, \tag{34}$$

where $j \geq 0$ and n are integers. These packets are built at future right null infinity, \mathcal{I}_R^+ , and peak at delayed exterior time, $u = 2\pi n/\epsilon$, with width $2\pi/\epsilon$. Therefore the vertical axis in Figure 7 has a discrete and intuitive physical interpretation, giving the counts of a particle detector sensitive to only frequencies within ϵ of $\omega_j = j\epsilon$, for a time $2\pi/\epsilon$ at $u = 2\pi n/\epsilon$. Late times correspond to large quantum number n (for the mirror Equation (5), late times have $u \approx 2t[1 + \mathcal{O}(\kappa t)^{-2/3}]$). For excellent time resolution, only one frequency bin is needed, where the particles pile up, $j = 0$, and a relatively large value of ϵ resolves the count in time. The text of Fabbri-Navarro-Salas [42] also describes the details needed to reconstruct Figure 7 by first packetizing the beta coefficient as done in Equation (34) and then secondly numerically integrating over ω' from 0 to ∞ , and third, computing the results, N_{jn} ,

$$N_{jn} = \int_0^{+\infty} d\omega' |\beta_{jn\omega'}|^2, \tag{35}$$

for each individual time bin, n , for a set frequency bin, j (in our fine-grained time resolution case, $j = 0$). While this numerical approach evolves the particle count in time, it is not particularly stream-lined, fast, nor arbitrarily accurate. In Section 6, we will find an analytic approach to the evolution process, resolving these issues.

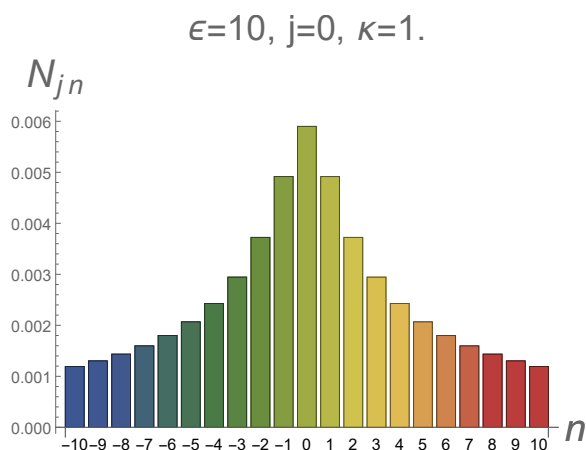


Figure 7. The particle count in time, via wave packet localization. The detector is set with $\epsilon = 10$, a relative large value ($\epsilon > 1$) in order to get clear time resolution. The scale of the system is $\kappa = 1$ and the frequency bin is in the lowest possible $j = 0$ value, where most of the particle production occurs, and finer resolution in time is possible. Notice there is no plateau, hence indicative of non-thermal radiation. This emission includes the ‘phantom radiation’ of soft particles as described in [17]. It is symmetric in delayed time, u , centered around time bin $n = 0$.

6. Analytic Time Evolution

The spectrum, Equation (25), is simple enough that analytical time evolution without discrete wave packetization is possible – possibly uniquely in the literature. Typically we would like to employ a Fourier transform converting from frequency to time. Since this does not work out in a straightforward manner, we consider that the Fourier transform of a radially symmetric function in the plane can be expressed as a Hankel transform. The Hankel transform, $N_u = H(N_\omega)/2$ —where by time symmetry we have divided the spectrum by 2 so that retarded time u ranges from $-\infty$ to $+\infty$ —is analytically tractable for the spectrum Equation (25):

$$\begin{aligned} \frac{384}{\kappa} N_u &= 5 {}_3F_2\left(\frac{7}{6}, \frac{3}{2}, \frac{11}{6}; 1, 2; -\frac{9}{16}u^2\kappa^2\right) \\ &+ 4 {}_3F_2\left(\frac{1}{2}, \frac{5}{6}, \frac{7}{6}; 1, 1; -\frac{9}{16}u^2\kappa^2\right) \\ &- 7 {}_3F_2\left(\frac{5}{6}, \frac{3}{2}, \frac{13}{6}; 1, 2; -\frac{9}{16}u^2\kappa^2\right). \end{aligned} \tag{36}$$

The particle spectrum dies off at large times as u^{-1} , so the total number indeed diverges.

Turning to the energy, a consistency check can be done by Hankel transforming the quantum of energy ωN_ω , and integrating over all time. The result for the transform, $E_u = H(\omega N_\omega)/2$, is

$$E_u = \frac{\sinh \theta}{3\sqrt{3}\pi\kappa u^3} - \frac{\cosh \theta}{3\sqrt{3}\pi u^2 \sqrt{9\kappa^2 u^2 + 16}}, \tag{37}$$

where $\theta \equiv \frac{1}{3} \sinh^{-1}(\frac{3\kappa u}{4})$. Equation (37) dies off as $u^{-8/3}$ for large times, so the total energy is finite. The result for the total energy by integrating over all time is also analytic,

$$E = \int_{-\infty}^{+\infty} E_u du = \frac{\kappa}{96}, \tag{38}$$

which agrees with the total energy as derived by the stress tensor, Equation (16), and the total energy as derived by integration of the particle spectrum with respect to frequency, Equation (33). As far as we know, this is the first solution for analytic time evolution of particle production from the quantum vacuum. Notice there is no need to resort to wavepacket discreteness as the creation is continuous. Nor have we made any analytic approximations. A plot of the evolution is given in Figure 8.

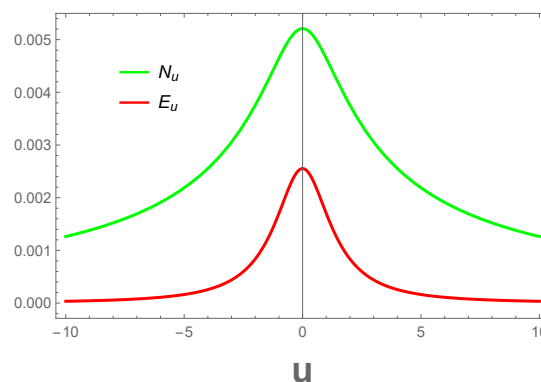


Figure 8. The continuous time evolution of particle creation, Equation (36), and time evolution of energy quanta, Equation (37). Here $\kappa = 1$ (though N_u/κ and E_u/κ^2 have invariant forms as a function of κu).

7. Conclusions

An interesting connection between the reality of the beta Bogoliubov coefficient, asymptotic inertia and finite energy, and mirror motion near the speed of light leads to particle radiation by quantum vacuum that is analytic in the energy flux, simple in the particle spectrum—an Airy function—and, remarkably, analytic expression of the time evolution of particle creation.

We evaluate the simplest allowed accelerated mirror with the needed conditions and derive all these physical quantities. The Airy mirror is asymptotically inertial, coasting at the speed of light; the total energy radiated is finite and simply $\kappa/96$ despite a soft particle divergence; the beta Bogoliubov coefficient is given by a real Airy-Ai function; the particle creation time evolution is analytic and exact.

The mirror has no horizon, and so there is no information loss. The finite energy corresponds to the black hole analog case where evaporation ceases, related to extremal black holes, remnants, or complete evaporation. The asymptotic inertia is responsible for finite energy, but inertial motions that asymptotically approach the speed of light do not preserve the interpretation of entanglement entropy derived from the rapidity as an adequate measure of unitarity (see Appendix C).

The radiated flux exhibits regions of negative energy flux (NEF); these are required by unitarity for the conditions present, and we expand on this “necessity of negativity” in the

Appendices, showing it follows directly from the asymptotically inertial nature. The lack of a horizon ensures information conservation although information loss does occur from an inertial horizon [39]. We further connect the NEF to the 1-D Schrödinger equation and interpretation of the rapidity as a Lorentz transformation and wavefunction in a potential well defined by the acceleration properties.

While obtaining a real, and simple, Bogoliubov coefficient is a significant advance, we further derive an analytic particle spectrum (integrating over the beta coefficient squared), time evolution (through a Hankel transform), and energy (further integrating over the spectrum times frequency). An exact analytic time evolution solution for particle production from the quantum vacuum may be unique in the literature. No discrete wave packetization is required (although we also show those results, consistent with the analytic one).

The techniques of accelerating boundary correspondences (ABC) and moving mirrors continue to deliver intriguing insights into connections between acceleration (or surface gravity), particle creation, and information. Furthermore, these lead to interesting directions for research in the properties of black holes (for which they serve as analogs) and quantum information, entanglement, and gravity.

Author Contributions: Both authors contributed equally to this work. Both authors have read and agreed to the published version of the manuscript.

Funding: Funding from state-targeted program “Center of Excellence for Fundamental and Applied Physics” (BR05236454) by the Ministry of Education and Science of the Republic of Kazakhstan is acknowledged. M.G. is also funded by the FY2018-SGP-1-STMM Faculty Development Competitive Research Grant No. 090118FD5350 at Nazarbayev University. E.L. is supported in part by the Energetic Cosmos Laboratory and by the U.S. Department of Energy, Office of Science, Office of High Energy Physics, under Award DE-SC0007867 and contract no. DE-AC02-05CH11231.

Conflicts of Interest: The authors declare no conflict of interest. The funders had no role in the design of the study; in the collection, analyses, or interpretation of data; in the writing of the manuscript, or in the decision to publish the results.

Appendix A. Necessity of Negativity

We emphasize that negative energy flux is a common, and indeed required [43], component of certain acceleration dynamics. That this follows from unitarity is discussed in [27] and references therein. Here we give two quick derivations.

From Equation (11) and the relations $f'(v) = e^{-2\eta}$ and $\alpha(v) = \eta'(v) e^\eta$, we can write

$$24\pi F(v) = -2e^{4\eta} [\eta'' + (\eta')^2] = -2e^{3\eta} \alpha'(v). \tag{A1}$$

This immediately implies

$$-12\pi \int_{-\infty}^{\infty} dv e^{-3\eta} F(v) = \int_{-\infty}^{\infty} dv \frac{d\alpha}{dv} = \alpha|_{-\infty}^{\infty}. \tag{A2}$$

Whenever the acceleration α vanishes asymptotically—as it does for any asymptotically inertial dynamics—(or if it is time symmetric), then the left hand side must be zero. Since $e^{-3\eta}$ is positive, then $F(v)$ must have negative regions.

This depends only on the conditions mentioned in the previous paragraph and not on the specific mirror trajectory used in this paper. One can also see this even more directly in terms of proper time τ :

$$12\pi F(\tau) = -\alpha'(\tau) e^{2\eta(\tau)}, \tag{A3}$$

so

$$12\pi \int d\tau e^{-2\eta} F(\tau) = - \int d\tau \frac{d\alpha}{d\tau}. \tag{A4}$$

Appendix B. Zero-Energy Resonance

The simple harmonic oscillator is the basis of many diverse physics areas. Here we consider a relation between particle radiation from an accelerated system and the oscillator equation. Let us adapt the usual form, $\ddot{\phi}(t) + \omega(t)\phi(t) = 0$ (in the time domain) or $\phi''(x) + k(x)\phi(x) = 0$ (in the space domain) and write it in terms of the light-cone coordinate retarded time $u = t - x$,

$$\psi''(u) + V(u)\psi(u) = 0. \tag{A5}$$

We allow the resonance frequency or spring constant to be spacetime dependent, and write it as $V(u)$ for reasons discussed below.

The immediate consequence (see also [43]) is that

$$\int_{-\infty}^{+\infty} du V(u)\psi(u) = - \int du \frac{d\psi'}{du}. \tag{A6}$$

This looks quite similar to Equation (A4). If ψ' vanishes at asymptotically early and late times, $|u| \rightarrow \infty$, then we find that for positive ψ the “potential” V must have negative regions.

Let us make the analogy more concrete. If $\psi(u) = e^{-\eta}$ then $-\psi'(u) = \alpha(u)$, which is the acceleration. While $\psi'(u) = -\alpha$, it is worth pointing out that $\psi(u)$ itself is the Lorentz transformation (LT) in retarded time from un-tilded to tilded boosted frame $\tilde{u} = e^{-\eta} u$, where the LT acts like a wave function. So our constraint on ψ' vanishing at infinity is exactly our condition in Appendix A, and the asymptotically inertial case we treat in the main text. Note that indeed ψ is always positive. Now the derivatives of η , and hence ψ , are also related through the Schwarzschild in Equation (10) to the energy flux $F(u)$ —which arises from the acceleration—through

$$V(u) \equiv 12\pi F(u) = -\frac{1}{2}\{p(u), u\} = \eta'(u)^2 - \eta''(u). \tag{A7}$$

Under these definitions, Equation (A6) is identical to Equation (A4). Thus, again we see the “necessity of negativity”.

The derivation in Appendix A relied on accelerating system dynamics while the one here arose from the simple harmonic oscillator equation. The harmonic oscillator can also be related to the 1-D Schrödinger equation

$$-\frac{\hbar^2}{2m}\psi'' + V\psi = E\psi, \tag{A8}$$

for a spacetime-dependent potential where the “spring constant”

$$k \leftrightarrow \frac{2m(E - V)}{\hbar^2}. \tag{A9}$$

Absorbing the \hbar and m factors, and taking the zero energy case, we see we can rewrite the Schrödinger equation as Equation (A5). Hence our $V(u) = 12\pi F(u)$ does act like a potential and $\psi(u)$ acts like a wave function. The moving mirror differential equation for energy flux, Equation (A7), and the zero-energy case with absorption of a negative sign into the definition of the potential, Equation (A8), corresponds to the physics of resonance transmission for a potential, $V(u) = V(-u)$, of a 1-D scattering threshold anomaly [44].

For the particular trajectory of the main text, we have the asymptotic condition $\psi' \rightarrow 0$ but to keep the wave function zero at infinity we perform a parity flip, $x \rightarrow -x$, on the mirror trajectory $f(v)$, Equation (3), resulting in

$$p(u) = u + \kappa^2 \frac{u^3}{3}. \tag{A10}$$

With $2\eta(u) = \ln p'(u)$, the rapidity $\eta(u) = \frac{1}{2} \ln(\kappa^2 u^2 + 1)$, hence asymptotically $+\infty$ rather than $-\infty$ without the parity flip, i.e., the mirror approaches an observer located at \mathcal{S}_R^+ at the speed of light, instead of receding at the speed of light as is the case with Equation (3). The wave function form is then

$$\psi(u) = \frac{1}{\sqrt{\kappa^2 u^2 + 1}}, \quad \psi(\pm\infty) = 0, \tag{A11}$$

plotted in Figure A1. The wave function is normalized by setting $\kappa = \pi$ so

$$\int_{-\infty}^{\infty} |\psi(u)|^2 du = 1. \tag{A12}$$

Plugging Equation (A10) into the Schwarzian relation, Equation (10), gives

$$F(u) = \frac{\kappa^2(2\kappa^2 u^2 - 1)}{12\pi(\kappa^2 u^2 + 1)^2}. \tag{A13}$$

which is PT symmetric $u \rightarrow -u$. Phrasing this as the potential $V(u) = 12\pi F(u)$ of the Schrödinger equation we see in Figure A1 how the wave function is localized within the potential well.

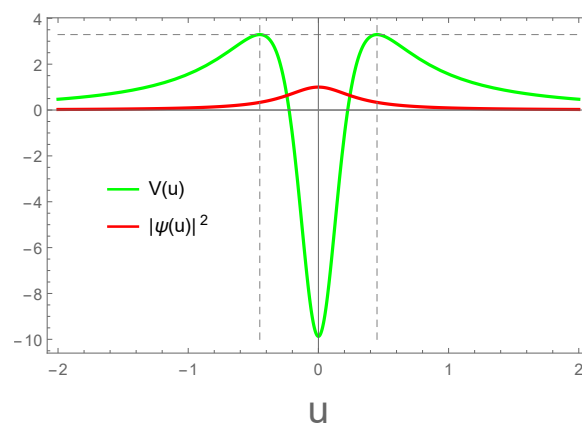


Figure A1. The potential Equation (A7) with Equation (A13), and the wave function Equation (A11). $|\psi^2|$ is normalized according to Equation (A12) where $\kappa = \pi$. The potential maxima occur at $u_m = \pm\sqrt{2}/\kappa$ with maximum value $V_m(u_m) = \kappa^2/3$; the zero crossings are at $u_0 = \pm 1/(\kappa\sqrt{2})$.

Appendix C. Entanglement Entropy and the Speed of Light

Entropy diverges because rapidity does, $S = -\eta/6$. Interestingly, a divergent information measure like entanglement entropy is, at first glance, seemingly at odds with the obvious unitarity of the dynamics as seen in the Penrose diagram. However, the entanglement-rapidity formula has a subtle caveat in that it was carefully derived [25,43,45–47] assuming unitarity a priori only in the cases where entropy (rapidity) achieves a constant non-infinite value in the far future. Since this is not the case for an asymptotic light speed moving mirror, the entropy as rapidity interpretation is not a good measure of unitarity [43] for such cases. This example highlights the need for caution because the entanglement as rapidity approach may not hold much utility for general motions that approach the speed of light, that is, for cases where $\eta \rightarrow \infty$.

References

1. Moore, G.T. Quantum Theory of the Electromagnetic Field in a Variable-Length One-Dimensional Cavity. *J. Math. Phys.* **1970**, *11*, 2679–2691. [CrossRef]
2. DeWitt, B.S. Quantum Field Theory in Curved Space-Time. *Phys. Rept.* **1975**, *19*, 295–357. [CrossRef]

3. Fulling, S.A.; Davies, P.C.W. Radiation from a moving mirror in two dimensional space-time: Conformal anomaly. *Proc. R. Soc. Lond. A Math. Phys. Sci.* **1976**, *348*, 393–414.
4. Davies, P.; Fulling, S. Radiation from Moving Mirrors and from Black Holes. *Proc. R. Soc. Lond. A Math. Phys. Sci.* **1977**, *A356*, 237–257. [[CrossRef](#)]
5. Unruh, W.G. Notes on black hole evaporation. *Phys. Rev. D* **1976**, *14*, 870. [[CrossRef](#)]
6. Johansson, J.R.; Johansson, G.; Wilson, C.M.; Nori, F. Dynamical Casimir Effect in a Superconducting Coplanar Waveguide. *Phys. Rev. Lett.* **2009**, *103*, 147003. [[CrossRef](#)]
7. Johansson, J.R.; Johansson, G.; Wilson, C.M.; Nori, F. Dynamical Casimir effect in superconducting microwave circuits. *Phys. Rev. A* **2010**, *82*, 052509. [[CrossRef](#)]
8. Johansson, J.R.; Johansson, G.; Wilson, C.M.; Delsing, P.; Nori, F. Nonclassical microwave radiation from the dynamical Casimir effect. *Phys. Rev. A* **2013**, *87*, 043804. [[CrossRef](#)]
9. Wilson, C.M.; Johansson, G.; Pourkabirian, A.; Simoen, M.; Johansson, J.R.; Duty, T.; Nori, F.; Delsing, P. Observation of the dynamical Casimir effect in a superconducting circuit. *Nature* **2011**, *479*, 376–379. [[CrossRef](#)]
10. Nation, P.D.; Johansson, J.R.; Blencowe, M.P.; Nori, F. Stimulating Uncertainty: Amplifying the Quantum Vacuum with Superconducting Circuits. *Rev. Mod. Phys.* **2012**, *84*, 1. [[CrossRef](#)]
11. Hawking, S. Particle Creation by Black Holes. *Commun. Math. Phys.* **1975**, *43*, 199–220. [[CrossRef](#)]
12. Walker, W.R.; Davies, P.C.W. An exactly soluble moving-mirror problem. *J. Phys. A Math. Gen.* **1982**, *15*, L477–L480. [[CrossRef](#)]
13. Good, M.R.R.; Anderson, P.R.; Evans, C.R. Mirror Reflections of a Black Hole. *Phys. Rev. D* **2016**, *94*, 065010. [[CrossRef](#)]
14. Good, M.R.; Ong, Y.C. Particle spectrum of the Reissner–Nordström black hole. *Eur. Phys. J. C* **2020**, *80*, 1169. [[CrossRef](#)]
15. Good, M.R.; Foo, J.; Linder, E.V. Accelerating boundary analog of a Kerr black hole. *arXiv* **2020**, arXiv:2006.01349.
16. Good, M.R.; Zhakenuly, A.; Linder, E.V. Mirror at the edge of the universe: Reflections on an accelerated boundary correspondence with de Sitter cosmology. *Phys. Rev. D* **2020**, *102*, 045020. [[CrossRef](#)]
17. Liberati, S.; Rothman, T.; Sonego, S. Nonthermal nature of incipient extremal black holes. *Phys. Rev. D* **2000**, *62*, 024005. [[CrossRef](#)]
18. Good, M.R. Extremal Hawking radiation. *Phys. Rev. D* **2020**, *101*, 104050. [[CrossRef](#)]
19. Rothman, T. Nonthermal nature of extremal Kerr black holes. *Phys. Lett. A* **2000**, *273*, 303–309. [[CrossRef](#)]
20. Foo, J.; Good, M.R. Hawking radiation particle spectrum of a Kerr–Newman black hole. *arXiv* **2020**, arXiv:2006.09681.
21. Good, M.R.R.; Yelshibekov, K.; Ong, Y.C. On Horizonless Temperature with an Accelerating Mirror. *JHEP* **2017**, *3*, 13. [[CrossRef](#)]
22. Good, M.R.; Ong, Y.C.; Myrzakul, A.; Yelshibekov, K. Information preservation for null shell collapse: A moving mirror model. *Gen. Rel. Grav.* **2019**, *51*, 92. [[CrossRef](#)]
23. Good, M.R. Spacetime Continuity and Quantum Information Loss. *Universe* **2018**, *4*, 122. [[CrossRef](#)]
24. Myrzakul, A.; Good, M.R. Unitary evaporation via modified Regge–Wheeler coordinate. In Proceedings of the 15th Marcel Grossmann Meeting on Recent Developments in Theoretical and Experimental General Relativity, Astrophysics, and Relativistic Field Theories, Rome, Italy, 1–7 July 2018.
25. Good, M.R.R.; Ong, Y.C. Signatures of Energy Flux in Particle Production: A Black Hole Birth Cry and Death Gasp. *JHEP* **2015**, *7*, 145. [[CrossRef](#)]
26. Good, M.R.R. *Reflecting at the Speed of Light*; World Scientific: Singapore, 2017; pp. 113–116. [[CrossRef](#)]
27. Good, M.R.; Linder, E.V.; Wilczek, F. Moving mirror model for quasithermal radiation fields. *Phys. Rev. D* **2020**, *101*, 025012. [[CrossRef](#)]
28. Good, M.R.R.; Linder, E.V.; Wilczek, F. Finite thermal particle creation of Casimir light. *Mod. Phys. Lett. A* **2020**, *35*, 2040006. [[CrossRef](#)]
29. Good, M.R.R.; Linder, E.V. Slicing the Vacuum: New Accelerating Mirror Solutions of the Dynamical Casimir Effect. *Phys. Rev. D* **2017**, *96*, 125010. [[CrossRef](#)]
30. Good, M.R.R.; Anderson, P.R.; Evans, C.R. Time dependence of particle creation from accelerating mirrors. *Phys. Rev. D* **2013**, *88*, 025023. [[CrossRef](#)]
31. Good, M.R.; Linder, E.V. Eternal and evanescent black holes and accelerating mirror analogs. *Phys. Rev. D* **2018**, *97*, 065006. [[CrossRef](#)]
32. Good, M.R.; Linder, E.V. Finite Energy but Infinite Entropy Production from Moving Mirrors. *Phys. Rev. D* **2019**, *99*, 025009. [[CrossRef](#)]
33. Sørensen, O. Exact Treatment of Interacting Bosons in Rotating Systems and Lattices. Ph.D. Thesis, Aarhus University, Aarhus, Denmark, 2012.
34. Birrell, N.; Davies, P. *Quantum Fields in Curved Space*; Cambridge Monographs on Mathematical Physics, Cambridge Univ. Press: Cambridge, UK, 1984. [[CrossRef](#)]
35. Carlitz, R.D.; Willey, R.S. Reflections on moving mirrors. *Phys. Rev. D* **1987**, *36*, 2327–2335. [[CrossRef](#)] [[PubMed](#)]
36. Walker, W.R. Particle and energy creation by moving mirrors. *Phys. Rev. D* **1985**, *31*, 767–774. [[CrossRef](#)] [[PubMed](#)]
37. Ford, L.; Roman, T.A. The Quantum interest conjecture. *Phys. Rev. D* **1999**, *60*, 104018. [[CrossRef](#)]
38. Ford, L.; Roman, T.A. Averaged energy conditions and quantum inequalities. *Phys. Rev. D* **1995**, *51*, 4277–4286. [[CrossRef](#)] [[PubMed](#)]
39. Good, M.; Abdikamalov, E. Radiation from an Inertial Mirror Horizon. *Universe* **2020**, *6*, 131. [[CrossRef](#)]

40. Nikishov, A.I. On vacuum vacuum amplitude and Bogolyubov coefficients. *J. Exp. Theor. Phys.* **2003**, *96*, 180–192. [[CrossRef](#)]
41. Good, M.R. On Spin-Statistics and Bogoliubov Transformations in Flat Spacetime With Acceleration Conditions. *Int. J. Mod. Phys. A* **2013**, *28*, 1350008. [[CrossRef](#)]
42. Fabbri, A.; Navarro-Salas, J. *Modeling Black Hole Evaporation*; Imperial College Press: London, UK, 2005.
43. Bianchi, E.; Smerlak, M. Entanglement entropy and negative energy in two dimensions. *Phys. Rev. D* **2014**, *90*, 041904. [[CrossRef](#)]
44. Senn, P. Threshold anomalies in one-dimensional scattering. *Am. J. Phys.* **1988**, *56*, 916–921. [[CrossRef](#)]
45. Myrzakul, A.; Xiong, C.; Good, M.R.R. Relativistic quantum information as radiation reaction: Entanglement entropy and self-force of a moving mirror analog to the CGHS black hole. *arXiv* **2021**, arXiv:2101.08139.
46. Fitkevich, M.; Levkov, D.; Zenkevich, Y. Dilaton gravity with a boundary: From unitarity to black hole evaporation. *arXiv* **2020**, arXiv:2004.13745.
47. Chen, P.; Yeom, D.H. Entropy evolution of moving mirrors and the information loss problem. *Phys. Rev. D* **2017**, *96*, 025016. [[CrossRef](#)]